

# A netrin domain-containing protein secreted by the human hookworm *Necator americanus* protects against CD4 T cell transfer colitis



GERALDINE BUITRAGO, DARREN PICKERING, ROLAND RUSCHER, CLAUDIA COBOS CACERES, LINDA JONES, MARTHA COOPER, ASHLEY VAN WAARDENBERG, STEPHANIE RYAN, KIM MILES, MATTHEW FIELD, KEITH DREDGE<sup>2</sup>, NORELLE L. DALY, PAUL R. GIACOMIN<sup>1</sup>, and ALEX LOUKAS<sup>1</sup>

CAIRNS, AND BRISBANE, AUSTRALIA

The symbiotic relationships shared between humans and their gastrointestinal parasites present opportunities to discover novel therapies for inflammatory diseases. A prime example of this phenomenon is the interaction of humans and roundworms such as the hookworm, *Necator americanus*. Epidemiological observations, animal studies and clinical trials using experimental human hookworm infection show that hookworms can suppress inflammation in a safe and well-tolerated way, and that the key to their immunomodulatory properties lies within their secreted proteome. Herein we describe the identification of 2 netrin domain-containing proteins from the *N. americanus* secretome, and explore their potential in treating intestinal inflammation in mouse models of ulcerative colitis. One of these proteins, subsequently named *Na*-AIP-1, was effective at suppressing disease when administered prophylactically in the acute TNBS-induced model of colitis. This protective effect was validated in the more robust CD4 T cell transfer model of chronic colitis, where prophylactic *Na*-AIP-1 reduced T-cell-dependent type-1 cytokine responses in the intestine and the associated intestinal pathology. Mechanistic studies revealed that depletion of CD11c+ cells abrogated the protective anticoliitic effect of *Na*-AIP-1. Next generation sequencing of colon tissue in the T-cell transfer model of colitis revealed that *Na*-AIP-1 induced a transcriptomic profile associated with the down-regulation of metabolic and signaling pathways involved in type-1 inflammation, notably TNF. Finally, co-culture of *Na*-AIP-1 with a human monocyte-derived M1 macrophage cell line resulted in significantly reduced secretion of TNF. *Na*-AIP-1 is now a candidate for clinical development as a novel therapeutic for the treatment of human inflammatory bowel diseases. (Translational Research 2021; 232:88–102)

<sup>2</sup>Current address: Zucero Therapeutics Ltd, Suite 1.11, Level 1, 1 Westlink Court, Brisbane, QLD 4076, Australia.

<sup>1</sup>These authors contributed equally.

From the Centre for Molecular Therapeutics, Australian Institute of Tropical Health and Medicine, James Cook University, Cairns, Queensland, Australia; Centre for Tropical Bioinformatics and Molecular Biology, Australian Institute of Tropical Health and Medicine, James Cook University, Cairns, Queensland, Australia; Zucero Therapeutics Ltd, Brisbane, Queensland, Australia.

Submitted for Publication January 14, 2021; received submitted February 23, 2021; accepted for publication February 25, 2021.

Reprint requests: Alex Loukas, and Paul R. Giacomini, Centre for Molecular Therapeutics, Australian Institute of Tropical Health and Medicine, James Cook University, McGregor Rd, Smithfield, Cairns, QLD 4878, Australia. e-mail: [Paul.Giacomini@jcu.edu.au](mailto:Paul.Giacomini@jcu.edu.au).

1931-5244/\$ - see front matter

© 2021 The Author(s). Published by Elsevier Inc. This is an open access article under the CC BY-NC-ND license (<http://creativecommons.org/licenses/by-nc-nd/4.0/>)

<https://doi.org/10.1016/j.trsl.2021.02.012>

**Abbreviations:** CD = Crohn's disease; DEGs = differentially expressed genes; DT = diphtheria toxin; DTR = diphtheria toxin receptor; ES = excretory secretory; HA = human albumin; H&E = hematoxylin and eosin; IBD = inflammatory bowel diseases; IL = interleukin; IMAC = immobilised metal ion affinity chromatography; i.p. = intraperitoneal; KEGG = Kyoto Encyclopaedia of Genes and Genomes; LFC = log fold change; MMP = matrix metalloprotease; Na-AIP-1 = *Necator americanus* Anti-Inflammatory Protein 1; NK = natural killer; PBS = phosphate buffered saline; PCA = principle component analysis; PMA = phorbol 12-myristate 13-acetate; TIMP = tissue inhibitor of metalloprotease; TNBS = trinitrobenzenesulfonic acid; TNF = tumour necrosis factor; UC = ulcerative colitis; WT = wild type;

## AT A GLANCE COMMENTARY

Buitrago, G et al.

### Background

Inflammatory bowel diseases (IBD) are debilitating and chronic conditions that are caused by uncontrolled inflammation in the intestine. Existing treatments are often poorly tolerated and minimally effective. In the search for new anti-inflammatory therapeutic modalities, we took inspiration from the co-evolution of humans parasitic worms (helminths).

### Translational Significance

Herein we show that gastrointestinal hookworms secrete a netrin protein that limits IBD symptoms and gut inflammation when delivered prophylactically in multiple mouse models of IBD. *Na-AIP-1* administration suppresses several inflammatory pathways within mouse gut tissue and a human macrophage cell line, and could be further developed as a safe and efficacious maintenance therapy for human IBD.

## INTRODUCTION

Inflammatory bowel disease (IBD) is a blanket term describing Crohn's disease (CD), ulcerative colitis (UC) and a handful of less common, but similarly debilitating, inflammatory conditions of the gastrointestinal tract. IBDs are chronic, refractory disorders that are classified in accordance with the nature of their respective immunological and pathological features; ultimately, the disorders are characterized by compromised epithelial barrier integrity and hyper-responsive inflammatory conditions. An increase in the incidence of IBDs in developing countries, combined with their existing prevalence in industrialized nations, has led to its emergence as a global disease of significant burden.<sup>1</sup> However, effective medical management of IBD remains elusive; whilst treatments exist, they are often poorly tolerated or of limited effect, underlining a need for the development of novel therapeutic modalities.

Various studies have documented the efficacy of live helminth infection in the alleviation of the signs and symptoms associated with inflammation in both human gastrointestinal inflammatory diseases and animal models of colitis.<sup>2–6</sup> Despite being well tolerated, inconsistent data has resulted from experimental human infection trials in patients with IBD,<sup>7–8</sup> and numerous hurdles complicate the adoption of live parasitic infection as a valid anti-inflammatory therapy.<sup>8</sup> As an alternative, the use of helminth-derived products has been explored.<sup>9</sup> Excretory/secretory (ES) products from the canine hookworm *Ancylostoma caninum* prevented inflammation in chemically induced TNBS colitis, a model of Crohn's disease where the pathology is driven by T-cell dependent mechanisms.<sup>10</sup> At termination, indicators of macroscopic inflammation and myeloperoxidase activity in the colons of *A. caninum* ES-treated mice showed significant abatement, accompanied by a reduction in the expression of Th1 cytokines and a skewing towards a modified Th2 environment. Hookworm ES products have also been shown to impart efficacy in a T cell-independent model of murine colitis,<sup>11,12</sup> as well as other mouse models of immune dysfunction diseases.<sup>13</sup> Together, these studies demonstrated the potential of therapeutic immunomodulation by hookworm ES products in the absence of live parasitic infection.

The characterization of the transcriptomes<sup>14,15</sup> and genomes<sup>16,17</sup> of several hookworm species has enabled deeper investigation into the components of the helminth secretome. Two of the most abundant proteins in the *A. caninum* secreted proteome – *Ac-AIP-1* and *Ac-AIP-2*<sup>18–21</sup> contain netrin domains and share sequence similarity with mammalian tissue inhibitors of matrix metalloproteases (TIMPs). Netrin domains are central to TIMPs and contain the active site N-terminal domain that confers MMP-inhibitory activity.<sup>22</sup> The hookworm TIMP-like proteins *AceES-2*<sup>23</sup> and *Ac-AIP-2*<sup>13</sup> display TIMP-like sequence and predicted structure, but lack defined residues involved in inhibition of MMP catalytic activity.<sup>23,24</sup> Moreover, netrin domains are involved in diverse processes from axonal guidance, morphogenesis and angiogenesis by regulating cell migration and survival.<sup>25</sup> Recombinant *Ac-AIP-2* was demonstrated to bind to mesenteric CD103+ dendritic cells and drive expansion of regulatory T cells (Tregs) that suppressed inducible asthma in mice and down regulated the expression of co-

stimulatory markers on human peripheral blood dendritic cells from asthmatic subjects.<sup>13</sup> The homologous *Ac*-AIP-1 protein was subsequently shown in recombinant form to suppress proinflammatory responses in the TNBS model of chemically-induced murine colitis.<sup>26</sup> Cantacessi and colleagues<sup>24</sup> identified several homologues of these TIMP-like proteins in helminths which primarily parasitize humans. It is plausible that, with humans as a natural host, netrin domain-containing proteins from these species may not only display anti-inflammatory properties, but may be better adapted to modulate human immune function. Accordingly, two potential netrin domain-containing proteins from the ES products of the major human hookworm, *Necator americanus*, were identified for further investigation. Herein we describe recombinant production of two novel netrin domain-containing proteins isolated from the *N. americanus* secretome, and the anti-colitic properties of one of them, *Na*-AIP-1, in acute and chronic models of colitis.

## MATERIAL AND METHODS

***N. americanus* netrin domain-containing proteins.** Netrin domain-containing proteins *Na*-AIP-1 and NECAME\_13168, from the intra-mammalian stages of *N. americanus*, were identified by Cantacessi et al.<sup>24</sup> Briefly, genome data for *N. americanus* was analyzed with known TIMP amino acid sequences from *Homo sapiens* (GenBank accession numbers XP\_010392.1, NP\_003246.1, P35625.1 and Q99727.1) and *Ac*-AIP-2 (EU523696.1) using BLASTp and InterProScan algorithms. TIMP-like proteins were then further assessed for an N-terminal signal peptide and netrin domain. Secondary structural predictions were conducted using MOLMOL 2K.1<sup>27</sup> and I-TASSER molecular graphics software.<sup>28</sup> *H. sapiens* TIMP-2 was the closest

homologue with known structure and accordingly this protein was used as the backbone on which to build the models (Fig 1).

**Recombinant protein expression.** cDNA sequences corresponding to the open reading frames (ORFs) were cloned without signal peptides (*Na*-AIP-1 residues 18 to 139; NECAME\_13168 residues 18 to 134) into the *Eco*RI and *Xba*I sites of the pPIC-Z-alpha plasmid (Invitrogen). Two extra base pairs were added to the C-terminal end of the sequences to maintain the reading frame and ensure translation of the c-myc and 6xHIS tags. These extra bp resulted in a glycine being added to the C-terminus upstream of the vector-derived tags within pPIC-Z-alpha. Recombinant proteins were expressed via secretion using the yeast *Pichia pastoris*. Recombinant proteins were isolated from the yeast culture supernatant using immobilized metal ion affinity chromatography (IMAC) on an ÄKTA FPLC chromatography system with a 5 mL HisTrap excel nickel column (GE Healthcare Life Sciences). Endotoxin removal was conducted using an EndoTrap HD Endotoxin Removal System (Hyglos) according to the manufacturer's instructions. Recombinant human albumin (HA) was expressed and purified in *P. pastoris* under identical conditions to the hookworm proteins, as indicated above.

**Mice and ethics.** Male BALB/c, male SJL/Jarc, male and female C57BL/6 mice and male B6.SVJ129-Rag1 (RAG KO) mice aged 5-7 weeks were obtained from Animal Resources Centre (Murdoch, Australia) or Australian BioResources (Moss Vale, Australia). Male and female C57BL/6.CD11c.DTR aged 6+ weeks, were bred in the JCU Small Animal Facility (Townsville, Australia). Mice were maintained in specific pathogen-free conditions in a temperature-controlled room with a 12 hour light/dark illumination cycle and received autoclaved food and water *ad libitum*. Animals were allowed

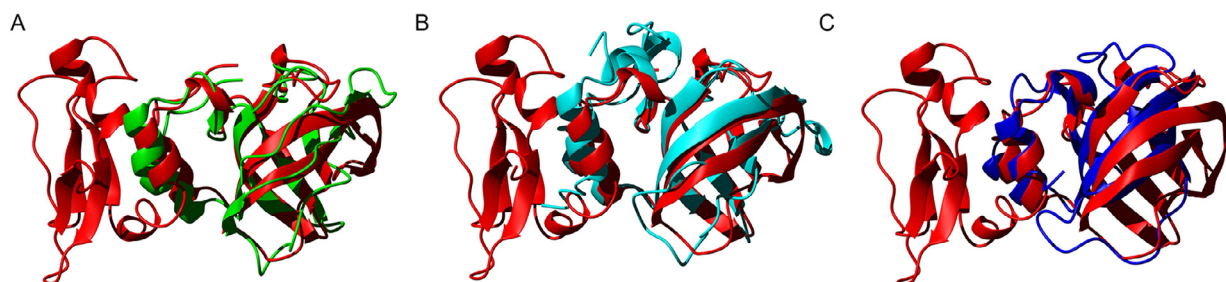


**Fig 1.** Superposition of hookworm TIMP-like proteins on human TIMP-2. *Necator americanus* *Na*-AIP-1 (Uniprot W2TPY4), NECAME\_13168 (W2SWZ9) and *Ancylostoma ceylanicum* AceES-2 (Q6R7N7, PDB code 3NSW) were modelled on the crystal structure of *Homo sapiens* TIMP-2 (Uniprot P16035; PDB code 1BR9). A, Superposition of *Na*-AIP-1 (green) on *H. sapiens* TIMP 2 (red) superimposed over residues 81-115 and 95-129 respectively. B, Superposition of NECAME\_13168 (aqua) on *H. sapiens* TIMP 2 superimposed over residues 81-100 and 96-115 respectively. C, Superposition of AceES-2 (blue) on *H. sapiens* TIMP-2 superimposed over residues 83-100 and 101-118, respectively. Modeling was conducted using Modeller and I-TASSER.28.

to adapt for 7 days before the commencement of experimental interventions. Mice were sacrificed via CO<sub>2</sub> asphyxiation. Experiments were approved by the James Cook University Animals Ethics Committee under Ethics Approval numbers A2012 and A2379 and conducted in accordance with National Health and Medical Research Council Australian Code for the Care and Use of Animals for Scientific Purposes (8th Edition, 2013) and in compliance with the Queensland Animal Care and Protection Act, 2001 (Act No.64 of 2001).

**Treatment administration.** Mice were randomly divided into treatment groups of 5 per cage, with an even split between sexes where relevant. *Na-AIP-1*, NECAME\_13168, HA control was administered by intra-peritoneal (i.p.) injection at a dose of 1 mg/kg body weight, in PBS vehicle (200  $\mu$ L total injection volume). The recombinant protein dosage level of 1 mg/kg and route of delivery was determined in consideration with results from similar studies.<sup>10–13</sup> Control mice received PBS vehicle only.  $\alpha$ IL12/23 mAb (clone C17.8, BioxCel) was administered at a dose of 1 mg/mouse per week.

**CD11c+ cell depletion.** C57BL/6 and C57BL/6.CD11c.DTR mice received 500 ng diphtheria toxin (Sigma-Aldrich) as indicated. Depletion of CD11c+ cells was confirmed by comparing CD3- CD19- CD11c+ MHCII+ cell frequency in the live mesenteric lymph node (mLN) cells between WT and DTR mice.

**TNBS-induced colitis.** Colitis was induced via intra-rectal injection of 100  $\mu$ L 1.5 mg TNBS in 50% EtOH in BALB/c mice, and 50  $\mu$ L 1.5 mg TNBS in 50% EtOH in SJL/Jarc mice, as described elsewhere.<sup>29</sup> TNBS administration was conducted on day zero of the experimental period unless otherwise indicated.

**T cell transfer colitis.** Colitis was induced in RAG KO mice using established protocols.<sup>30–31</sup> Briefly, spleens were harvested from C57BL/6 WT donor mice and CD4+ cells were isolated by negative selection via magnetic separation, using the EasySep CD4+ T Cell Isolation kit (Stemcell Technologies) as per manufacturer's instructions. Enriched CD4 cells were labeled with APC-anti-mouse CD4 (clone RM4-5; BD Biosciences) and FITC-anti-mouse CD25 (clone AL-21; BD Biosciences) and sorted into CD4+ CD25- fractions on a BD FACSAria III. Each RAG KO mouse received 100  $\mu$ L of PBS containing  $4 \times 10^4$  purified CD4+ CD25- cells by i.p. injection on day 0. Naïve control RAG KO mice did not receive donor CD4 cells.

**Clinical and macroscopic disease scores.** Mice were assessed daily (TNBS experiments) or twice weekly (T cell transfer experiments) for clinical signs of disease and scored using criteria adapted from Ruysers et al.<sup>10</sup> Piloerection and lethargy, diarrhea and rectal thickening/bleeding were graded according to severity from 0

(absent) to 2 (severe), to a maximum cumulative total score of 6. At necropsy, colons were removed, flushed with PBS and assessed for length and macroscopic signs of disease utilizing criteria adapted from Ruysers et al.<sup>10</sup> Adhesion, edema and thickening were graded according to severity from 0 (absent) to 2 (severe), and ulceration was graded from 0 (absent) to necrosis (3), to a maximum cumulative total score of 9.

**Histological analysis of distal colon tissue.** Distal colon tissue was harvested in 1 cm sections and fixed in 4% formalin overnight, whereupon tissue was transferred to 70% EtOH. Embedding of tissue in paraffin, hematoxylin and eosin (H/E) staining was performed at the QIMR Berghofer Medical Research Institute histology facility (Brisbane, Australia) or the Advanced Analytical Centre, James Cook University (Cairns, Australia). Photomicrographs of tissue sections were scored by a researcher blinded to experimental group on a scale of 0-5 for each of the following parameters; (1) epithelial pathology (crypt elongation, hyperplasia, and erosion), (2) mural inflammation and (3) edema for an overall maximal total histology score of 15.

**Cytometric bead array (CBA).** Cytokine detection was conducted on whole colon tissue homogenate (500  $\mu$ L PBS/1 cm tissue) using a BD Mouse Inflammation CBA kit (BD Biosciences), as per the manufacturer's instruction. Visualization and analysis of CBA was conducted using FCAP Array software version 3.0.

**Gene expression analysis.** In a representative T cell transfer experiment, groups of 4 mice treated with either PBS,  $\alpha$ IL12/23 or *Na-AIP-1* were sacrificed at day 27 and colon tissues processed for RNAseq analysis. At termination, colons were removed and cleaned in sterile PBS. One cm sections of distal colon were collected into RNAlater (Sigma-Aldrich) on ice. Total RNA was extracted from macerated whole colon tissue using the RNeasy Plus Mini Kit (QIAGEN) according to the manufacturer's protocol and stored at  $-80^{\circ}$ C. Sequencing libraries were prepared using TruSeq Stranded mRNA Library Prep Kit (Illumina) and sequenced by the Australian Genomics Research Facility (AGRF, Melbourne, Australia). Paired-end sequencing to generate a read length of 150 bp was conducted using NovaSeqS4. Adapter sequences were trimmed using Cutadapt version 1.91<sup>32</sup> and trimgalore version 0.5.0\_dev ([https://www.bioinformatics.babraham.ac.uk/projects/trim\\_galore/](https://www.bioinformatics.babraham.ac.uk/projects/trim_galore/)). Data quality control was performed using FastQC (<https://www.bioinformatics.babraham.ac.uk/projects/fastqc/>). STAR version 2.7.0a<sup>33</sup> was utilized for read alignment, with alignment to the murine reference genome mm10 ([ftp.ensembl.org/pub/release-90/fasta/mus\\_musculus/dna/](ftp.ensembl.org/pub/release-90/fasta/mus_musculus/dna/)). Data normalization using EDASeq version 2.20.,<sup>34</sup> RUV correction,<sup>35</sup> principle component analysis (PCA), and differential gene expression analysis



were conducted using the consensusDE version 1.4.0 package<sup>36</sup> in R version 3.6.2, and results from edgeR version 3.28.0<sup>37</sup> are reported. When assessing differentially expressed genes (DEGs), those with a log<sub>2</sub>-fold change (LFC) of  $-0.5$  to  $0.5$  were excluded. An edgeR FDR-adjusted  $P$  value  $<0.05$  was considered significant.<sup>38</sup> Differential gene expression analyses were conducted between colitic mice receiving PBS, colitic mice receiving  $\alpha$ IL12/23, and colitic mice receiving *Na*-AIP-1. Volcano plots depicting DEGs were constructed in R using plotting functions in the graphics package version 3.6.2.

**THP-1 derived M1 macrophages.** M1 macrophages derived from the human THP-1 monocyte cell line were obtained as described elsewhere<sup>39</sup> with some modifications. THP-1 cells were resuspended in R-10 medium containing 200 nM phorbol 12-myristate 13-acetate (PMA) (Sigma) and cultured at  $1 \times 10^5$  cells per 100  $\mu$ L per well in flat-bottom 96-well plates. After 48 hours the cells were washed with PBS and the medium replaced with R-10 (without PMA). After 24 hours of PMA starvation, the resulting M0 macrophages were polarized by replacing the medium with R-10 containing 20 ng/mL human recombinant IFN $\gamma$  and 2 ng/mL human recombinant TNF (PeproTech). Forty-eight hours later the cells were washed and the media replaced with R-10 containing either 100  $\mu$ g/mL *Na*-AIP-1 or an equivalent volume of PBS (vehicle control). The cells were stimulated with 10 ng/mL LPS (Sigma) and soups were collected 24 hours later and analysed using a LEGENDplex (BioLegend) kit.

**Statistical analyses.** Statistical analyses were conducted using GraphPad Prism 8 software. Comparisons between all groups were conducted using unpaired, one-way ANOVA (Holm Sidak) unless otherwise specified. Comparisons between individual groups were performed by unpaired, two-way Mann-Whitney U tests (Holm Sidak), vs negative/vehicle control, unless otherwise specified. Comparisons between all groups at multiple time points were conducted using unpaired, two-way ANOVA (Holm Sidak) unless otherwise specified. Comparisons between individual groups were performed by unpaired, two-way Mann-Whitney U tests (Holm Sidak), vs negative/vehicle control, unless otherwise specified. Significance levels were set at a  $P$  value of  $\leq 0.05$ .

## RESULTS

**Netrin domain-containing proteins of *N. americanus*.** TIMP-like proteins *Na*-AIP-1 and NECAME\_13168, from the infective L3 stage of *N. americanus*, were identified by Cantacessi et al.<sup>24</sup> Briefly, genome data for *N. americanus* was analyzed with known TIMP

amino acid sequences from *Homo sapiens* (GenBank accession numbers XP\_010392.1, NP\_003246.1, P35625.1 and Q99727.1) and *Ac*-AIP-2 (EU523696.1) using BLASTp and InterProScan algorithms. TIMP-like proteins were then further assessed for an N-terminal signal peptide and netrin domain. Netrin domains are central to TIMPs and contain the active site N-terminal domain that confers MMP-inhibitory activity.<sup>22</sup> The hookworm TIMP-like proteins *Ace*ES-2<sup>23</sup> and *Ac*-AIP-2<sup>13</sup> display TIMP-like sequence and predicted structure, but lack defined residues involved in inhibition of MMP catalytic activity.<sup>23,24</sup> *H. sapiens* TIMP-2 was the closest homologue with known structure and accordingly this protein was used as the backbone on which to build the models (Fig 1).

**Expression of recombinant *N. americanus* proteins.** Recombinant *Na*-AIP-1 migrated at the expected size (377 bp, 16.2 kDa) of the mature protein after proteolytic processing of the signal peptide under denaturing and reducing conditions (Figure S1). Yeast culture supernatant of 500 mL produced a yield of recombinant *Na*-AIP-1 of 47.4 mg with an endotoxin concentration of 0.74 EU/mg protein, and a yield of recombinant NECAME\_13168 of 11.4 mg with an endotoxin concentration of 3.73 EU/mg protein. Both proteins had endotoxin concentrations that were within the limits of cell culture applications.

**Prophylactic delivery of recombinant *Na*-AIP-1 limits clinical and pathological determinants of TNBS-induced colitis.** To examine the potential efficacy of *Na*-AIP-1 and NECAME\_13168 in murine colitis, we first employed an 8-day model of acute TNBS-induced colitis. BALB/c mice received i.p. injections of *Na*-AIP-1, NECAME\_13168 or HA on days -1, 2 and 5 and were challenged twice by intrarectal administration of TNBS on days 0 and 6, and sacrificed at day 8 (Fig 2, A). The rationale of double TNBS administration was used in consideration with established protocols, and employed to reflect in a more robust fashion the active and remitting nature of colitic Th1 inflammation observed in human CD.<sup>40-41</sup> Furthermore, this approach enabled the characterization of treatment efficacy in both acute ( $<48$  hours postchallenge) and subacute ( $>48$  hours postchallenge) conditions. Mice treated with HA experienced rapid bodyweight loss within 48 hours of TNBS administration, followed by a slow recovery of weight (Fig 2, B). While treatment of mice with NECAME\_13168 did not affect this weight loss, treatment with *Na*-AIP-1 resulted in significantly reduced initial weight loss and a rapid recovery of weight by day 3, similar to mice treated with  $\alpha$ IL12/23 mAb (Fig 2, B). *Na*-AIP-1 and  $\alpha$ IL12/23 mAb also displayed reduced weight loss compared to HA control mice after the second TNBS administration. Consistent with protection against weight loss, mice treated with *Na*-AIP-1 or  $\alpha$ IL12/23 also

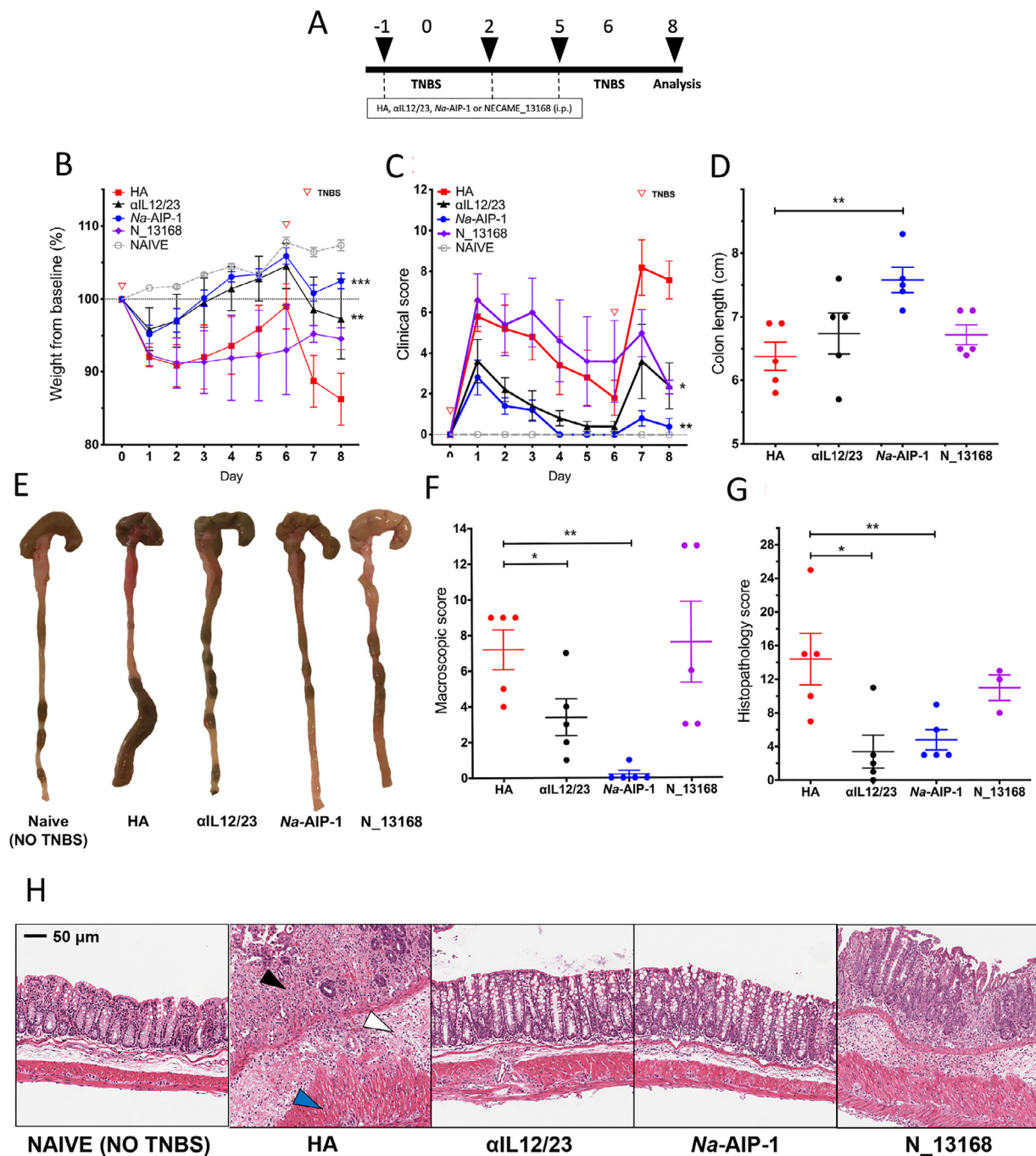


**Fig 2.** Prophylactic delivery of recombinant Na-AIP-1 limits clinical and pathological determinants of TNBS-induced colitis. **A**, Mice received intraperitoneal injections of 1 mg/kg body weight of Na-AIP-1, NECAME\_13168 (N\_13168) or recombinant human albumin (HA) control on days -1, 2 and 5.  $\alpha$ IL12/23 mAb (clone C17.8, BioxCell) was administered at a dose of 1 mg/mouse per week. Mice were received an intrarectal administration of TNBS on days 0 and 6. **B**, Relative change in body weight compared to baseline. **C**, Clinical scores of colitis. **D**, Colon length at termination. **E**, Representative images of colon tissue in each group. **F**, Macroscopic scores of colon tissue pathology. **G**, Blinded histological scoring of distal colon tissue pathology. **H**, Representative photomicrographs of H&E stained distal colon sections from each group. Annotations indicate inflammatory pathology, including loss of normal epithelial barrier structure (black arrow), lymphocytic infiltration of the lamina propria (white arrow) and thickening of the muscularis (blue arrow). Experiment was performed twice (n=5 per treatment group); representative results from a single experiment are shown. Data are presented as mean  $\pm$  SEM. Comparisons were conducted using one-way ANOVA (Holm-Sidak), two-way ANOVA or Mann Whitney t test (nonparametric) where appropriate, \* $P \leq 0.05$ , \*\* $P \leq 0.01$ , \*\*\* $P \leq 0.001$  compared to HA group.

exhibited significantly reduced clinical indicators of disease compared to HA-treated mice, while NECAME\_13168 was not protective (Fig 2, C). We next examined the effect of *Na*-AIP-1 and NECAME\_13168 on macroscopic and histological pathology in the colon upon termination of the TNBS experiment. Consistent with reduced colitis, mice treated with *Na*-AIP-1 displayed significantly longer colons than HA treated mice (Fig 2, D), where colons visually appeared similar to the appearance of naïve mice that were not treated with TNBS (Fig 2, E). Macroscopic scoring of inflammatory pathology revealed that both *Na*-AIP-1 and  $\alpha$ IL-12/23, but not NECAME\_13168, significantly reduced macroscopic pathology compared to the HA group (Fig 2F). Similarly, blinded analysis and scoring of distal colon tissue sections demonstrated that  $\alpha$ IL-12/23 and *Na*-AIP-1 treatment significantly reduced colon histopathology scores compared to HA control mice (Fig 2, G). While mice treated with HA or NECAME\_13168 displayed considerable morphological corruption, with diffuse transmural lymphocytic infiltration, disruption of normal epithelial barrier integrity and loss of goblet cells, mice receiving *Na*-AIP-1 or  $\alpha$ IL12/23 displayed normalized colon appearance, similar to naïve mice (Fig 2, H). Together, these data suggest that prophylactic delivery of *Na*-AIP-1 is effective at limiting disease in acute TNBS colitis, similar to IL-12/23 neutralization, an approved human colitis therapy.<sup>42</sup>

We next examined whether *Na*-AIP-1 exerts similar efficacy when delivered therapeutically, that is, after disease onset has occurred. To do this, we employed a short 3-day colitis model, where BALB/c mice were challenged with intrarectal TNBS on day 0, and treated with *Na*-AIP-1 i.p. on either day -1 (prophylactic) or day 1 or day 2 (therapeutic) (Fig S3A). As expected, prophylactic delivery of *Na*-AIP-1 was able to reduce weight loss, clinical score and increase colon length compared to mice treated with PBS vehicle only (Fig S3B-D). Therapeutic treatment of mice with *Na*-AIP-1 one day after TNBS resulted in a similar level of protection to prophylactic treatment, but treatment at day 2 did not result in any suppression of disease parameters compared to PBS treatment (Fig S3B-D). These results suggest that *Na*-AIP-1 has limited therapeutic ability to suppress active colitis and may be most effective when provided therapeutically.

***Na*-AIP-1 limits gut pathology and inflammatory responses in a T-cell transfer model of colitis.** We next examined whether *Na*-AIP-1 also displayed efficacy at limiting disease in a more chronic, immunologically driven model of colitis that closely mirrors human disease.<sup>43</sup> We employed a T cell transfer model of colitis where C57BL/6 RAG KO mice received CD4+ CD25-cells from wildtype C57BL/6 mice i.p, a model used in multiple previous studies where the transferred cell

populations are a mixture of naïve and non-Treg memory T cells.<sup>31,44-46</sup> Mice were treated with either *Na*-AIP-1 or HA control twice per week (Fig 3, A). Control mice received  $\alpha$ IL12/23 mAb once per week, which has been shown to suppress T cell transfer colitis,<sup>43</sup> and naïve control mice received no cell transfer. As expected, treatment of mice with the negative control protein HA displayed signs of colitis starting at day 21, including weight loss between days 18-25 (Fig 3, B) and increased clinical signs of disease that peaked at day 25 (Fig 3, C). In contrast, mice treated with  $\alpha$ IL12/23 or *Na*-AIP-1 did not lose weight and had significantly reduced clinical scores compared to HA control mice (Fig 3, B-C). Consistent with reduced induction of colitis, the colons of mice receiving  $\alpha$ IL12/23 or *Na*-AIP-1 were significantly longer than those of HA-treated mice (Fig 3, D) and displayed lessened macroscopic evidence of colitis, such that colons resembled those of naïve mice (Fig 3, E). Blinded grading of distal colon tissue sections demonstrated that  $\alpha$ IL12/23 or *Na*-AIP-1 treatment significantly reduced colon histopathology scores compared to HA control mice (Fig 3F), where HA-treated mice displayed epithelial hyperplasia, dense leukocyte infiltration in the lamina propria, and goblet cell loss that was not observed in  $\alpha$ IL12/23 or *Na*-AIP-1-treated mice (Fig 3, G).

**Targeted depletion of CD11c+ cells limits the anti-inflammatory influence of *Na*-AIP-1.** Since the homologous *Ac*-AIP-2 protein is known to utilize mesenteric DCs in the suppression of induced asthma,<sup>13</sup> we next assessed whether ablation of CD11c+ cell populations would inhibit the function of *Na*-AIP-1 in an inflammatory setting. We utilized mice engineered to express a high-affinity simian diphtheria toxin receptor on CD11c-bearing cells (CD11c-DTR), enabling targeted depletion of these cells by administration of human diphtheria toxin. Mice were then subjected to a 9-day TNBS colitis protocol (Fig 4, A). Recombinant *Na*-AIP-1 or HA treatment was delivered 24 hour prior and 24 hour post each TNBS challenge. All mice received 500 ng of diphtheria toxin on days -1, 4, and 8 to ensure consistent depletion of CD11c+ macrophages and dendritic cells, which was confirmed by flow cytometric analysis of reduced CD11c+ MHCII+ cells in the mLN of DTR+ mice (Fig 4, B). As expected, TNBS administration to WT mice and treatment with HA control resulted in rapid weight loss (Fig 4, C) and increased clinical score (Fig 4, D) that was slow to subside, and similar to that seen in CD11c+ cell-depleted DTR+ mice. Also as expected, *Na*-AIP-1 treatment of CD11c-sufficient WT mice resulted in rapid recovery from weight loss, and reduced clinical scores between days 5-6 post-TNBS compared to the control group, although low sample size prevented statistical significance. However, *Na*-AIP-1 did not protect against

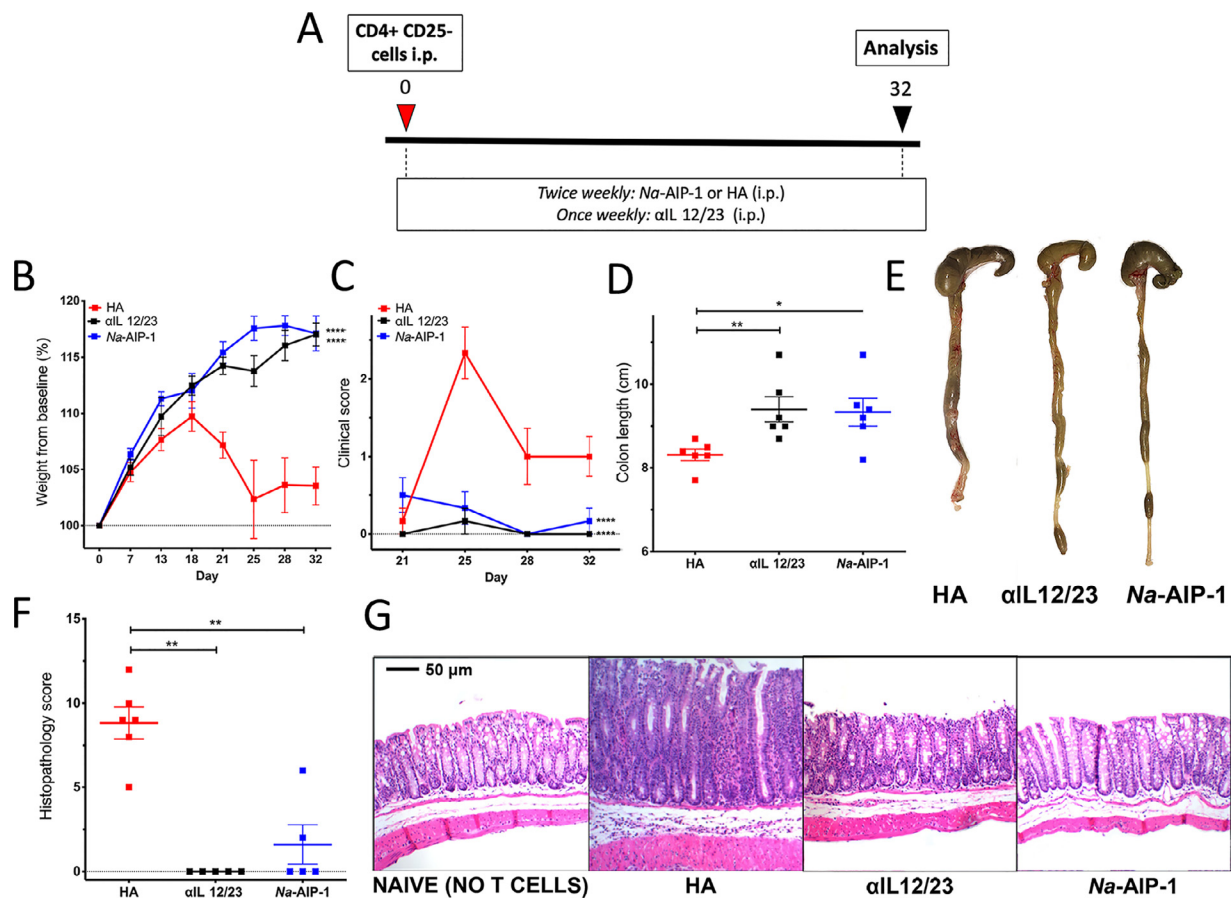


**Fig 3.** Na-AIP-1 limits gut pathology and inflammatory T cell responses in a T cell transfer model of colitis. A, Mice were injected with  $4 \times 10^4$  CD4+ CD25- T cells via intraperitoneal (i.p.) injection on day 0, and were treated twice weekly with either Na-AIP-1 or HA control, or  $\alpha$ IL12/23 mAb once weekly via i.p. injection. B, Relative change in body weight compared to baseline. (C, Clinical scores of colitis. D, Colon length at termination. E, Representative images of colon tissue in each group. F, Blinded histological scoring of distal colon tissue pathology. G, Representative photomicrographs of H&E stained distal colon sections from each group. Data are presented as mean  $\pm$  SEM. Experiment was performed three times ( $n = 5$  per treatment group); representative results from a single experiment are shown. Comparisons were conducted using two-way RM ANOVA (Holm-Sidak) or Mann Whitney t-test (nonparametric) where appropriate. \*  $P \leq 0.05$ , \*\*  $P \leq 0.01$ , \*\*\*\*  $P \leq 0.0001$  compared to HA group.

weight loss and clinical disease in CD11c-depleted DTR mice (Fig 4, C-D). These results were consistent with terminal colon length and macroscopic score parameters, which showed that Na-AIP-1 administration significantly protected against colon shortening (Fig 4, E) and macroscopic disease (Fig 4, F) in WT mice, but not in CD11c-depleted DTR mice. Visual inspection of the colons of mice at termination highlighted the striking disparity between Na-AIP-1 (WT) and Na-AIP-1 (DTR) mice, with the latter showing high degrees of edema and distal necrosis (Fig 4, G). The outcome of these studies suggests Na-AIP-1 requires the presence of CD11c+ cells in order to exert an anticolic effect in the TNBS model.

**Differentially expressed genes in the colon of mice treated with Na-AIP-1 during T cell transfer colitis.** We next

aimed to further investigate the potential mechanism of action of Na-AIP-1 during colitis by investigating the colon tissue-specific biological effects in treated mice using RNA sequencing, and comparing with  $\alpha$ IL12/23 treatment where the mechanism of action is well understood. We employed the same T cell transfer model of colitis as described in Fig 3, however in this experiment mice were sacrificed at day 27 when all PBS vehicle control-treated mice showed clinical indications of colitis, but Na-AIP-1-treated and  $\alpha$ IL12/23-treated mice displayed limited disease (Fig S2). The PCA plot exhibits a clear separation in gene expression profiles between treatment groups, and recognizable clustering of biological replicates within treatment groups (Fig 5, A). In order to determine the magnitude of transcriptional alterations generated in T cell transfer colitis, we measured



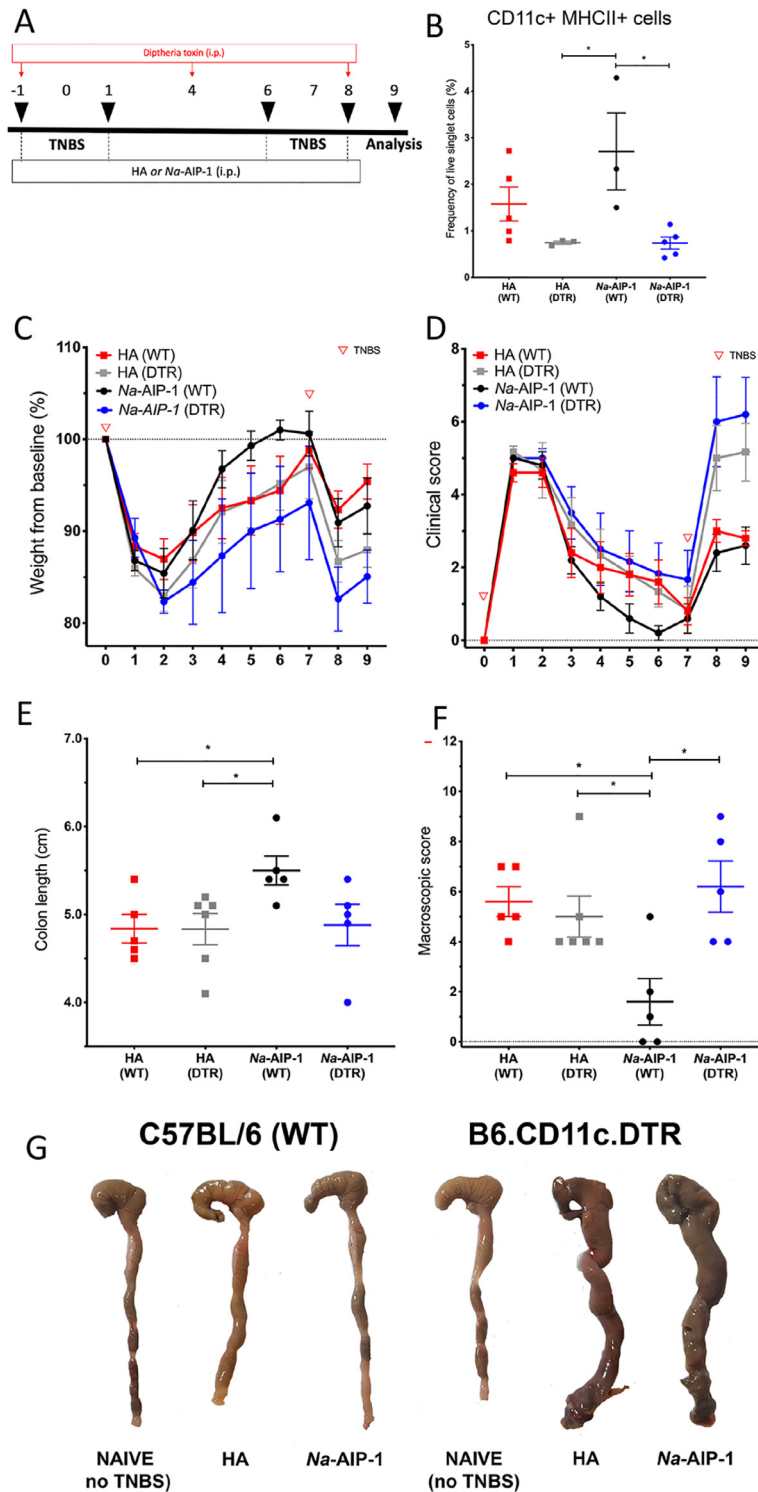


**Fig 4.** Targeted depletion of CD11c+ cells limits the anti-inflammatory influence of Na-AIP-1 in TNBS colitis. A, Beginning on day -1, C57BL/6 WT or CD11c-DTR mice were treated intraperitoneally with either Na-AIP-1 or HA control and challenged twice by intrarectal administration of TNBS on days 0 and 7. B, CD11c+ cells were depleted by diphtheria toxin (DT) treatment, which was confirmed by flow cytometry analysis of frequencies of CD11c+MHCII+ cells in the mesenteric LN. C, Relative change in body weight compared to baseline. D, Clinical scores. (E, Colon length at termination. F, Macroscopic scores of colon tissue pathology. G, Representative images of colon tissue in each group. Data are presented as mean  $\pm$  SEM; \*  $P \leq 0.05$  compared to Na-AIP-1-treated WT, two-way unpaired Mann-Whitney test. Experiment was performed three times (n = 5 per treatment group, n = 2 per naïve group); representative results from a single experiment are shown.

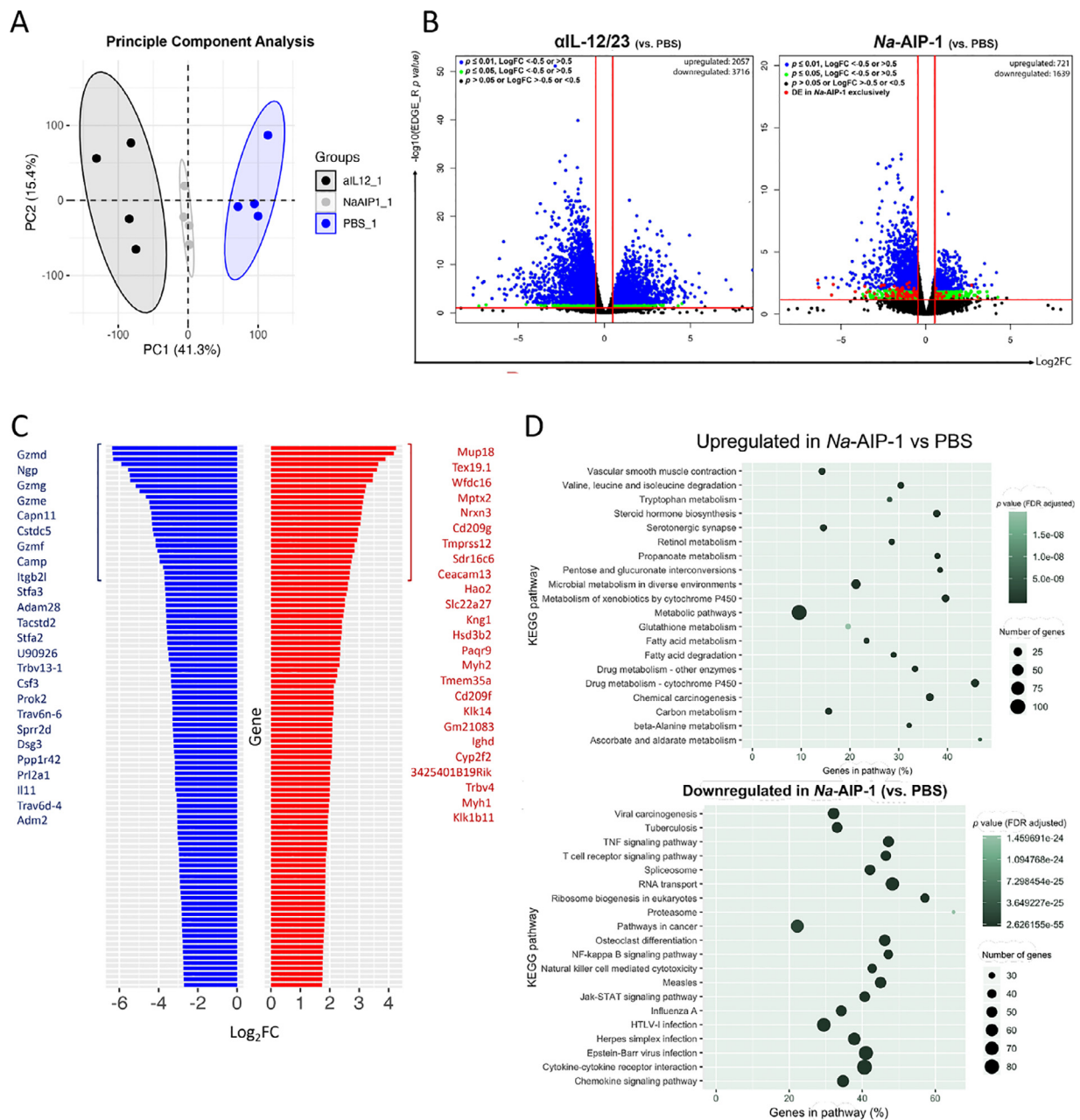


**Fig 5.** RNAseq profiling of differentially expressed genes in the colons of mice treated with Na-AIP-1 during T cell transfer colitis. Colitis was induced in RAG KO mice by adoptive transfer of CD4+ CD25- T cells on day 0. Mice received PBS, αIL12/23 or Na-AIP-1 twice per week by intraperitoneal injection. Termination was conducted at day 27, when all vehicle control (PBS) mice displayed clinical indicators of colitis. RNA-seq was conducted on distal colon sections and transcriptomic expression profiles compared. A, PCA exhibits a clear separation in gene expression profiles between treatment groups, recognisable clustering of biological replicates within treatment groups, and a distinct separation between treatment groups. B, Comparison of αIL12/23 expression with the vehicle control identified 5,773 DEGs, of which 64% were downregulated. Prophylactic administration of Na-AIP-1 induced 2,360 DEGs, of which 69% were downregulated in comparison to the PBS control. Data and images were generated using the consensusDE package in R.38 (C) Bar chart illustrating the top 25 downregulated (blue) and upregulated (red) DEGs in Na-AIP-1-treated mice compared to PBS. D, Top 20 KEGG pathways associated with genes differentially expressed in Na-AIP-1-treated mice compared to PBS. Only pathways with ≥2 hits have been included to ensure biological relevance. Terms are listed by rank. Frequency of all DEGs within the treatment group that are annotated to the respective term are represented as genes in pathway (%). Images were constructed in R using plotting functions in the graphics package version 3.6.2. or ggplot2\_3.2.1.52 Ellipses represent 80% confidence level. Results from a single experiment are shown (n = 4 per treatment group).

differential gene expression between mice receiving  $\alpha$ IL12/23p40 antibody, the benchmark for the induction of remission in the adoptive transfer model of murine colitis,<sup>43</sup> to the PBS-treated control. This comparison revealed 2057 upregulated genes and 3716 significantly downregulated genes in  $\alpha$ IL12/23 mice compared to PBS treated mice (Fig 5, B). When comparing the transcriptional profile of mice treated with *Na*-AIP-1 to the PBS vehicle control, a total of 2,360 genes were differentially expressed. Of these, 721 genes were significantly upregulated and 1639 were significantly downregulated (Fig 5, B). Four of the top 7 most highly downregulated genes in the gut of *Na*-AIP-1-treated mice were granzymes (Fig 5, C), programmed cell death-inducing serine proteases released by cytoplasmic granules within cytotoxic T cells and NK cells. This was reflected in the KEGG pathway analysis where differentially expressed genes were significantly enriched for NK cell-mediated cytotoxicity, as well as related pathways such as NF-kappa B signaling, TNF signaling, T-cell receptor signaling and cytokine-cytokine receptor signaling pathways were also significantly downregulated (all FDR adjusted *P*-values < 0.05; Fig 5, D). KEGG pathways that were significantly upregulated in *Na*-AIP-1-treated mice compared to PBS-treated colitic mice received lower *P* values and generally had fewer genes affected within each pathway (Fig 5, D). Moreover, many of the upregulated pathways in *Na*-AIP-1-treated mice were involved in various metabolism processes, amino and fatty acid degradation processes, and steroid hormone biosynthesis. Two of the most highly upregulated genes in *Na*-AIP-1-treated mice were the dendritic cell C-type lectin receptors, *Cd209g* and *Cd209f* (Fig 5, C). Comparison of DEGs between mice treated with *Na*-AIP-1 and  $\alpha$ IL-12/23 revealed 20 genes in which transcription was upregulated by *Na*-AIP-1 but not  $\alpha$ IL12/23, and 76 genes in which transcription was exclusively downregulated by *Na*-AIP-1 (Fig S4). Genes which underwent the greatest change in expression levels that were exclusive to *Na*-AIP-1 were dominated by a downregulation in those related to cytotoxic T cell and NK cell granulation (*Gzmd*, *Gzng*, *Gzmf*) and T cell receptor alpha chain components (*Trav6n-6*, *Trav9d-3*, *Trav9n-3*, *Trav14n-3*). Genes with a log fold change (LFC) between 1 and -1 were excluded to ensure biological relevance.

***Na*-AIP-1 reduces expression of TNF signaling pathway genes in mouse and human tissues.** Genes involved in the TNF signaling pathway (KEGG mmu04668) were analyzed from the RNA-seq dataset for mice treated with *Na*-AIP-1 and vehicle. Almost half the genes in this pathway (43 genes), including *Tnf* and other inflammatory cytokines such as *Il6* and *Il1*, underwent significant downregulation when log<sub>2</sub> fold-change was analyzed using EDGE\_R (Fig 6, A). To determine whether suppression of TNF was also detected in

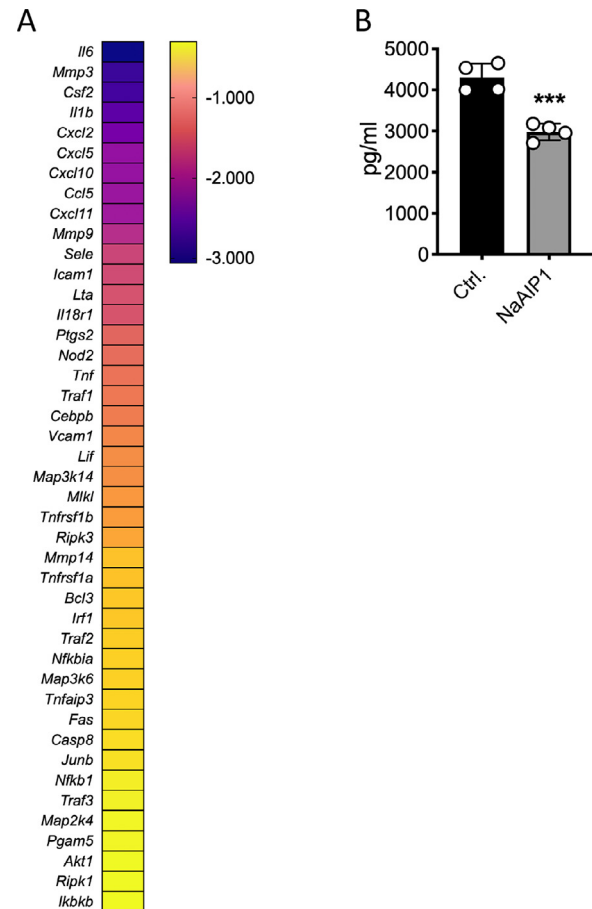


**Fig 6.** *Na*-AIP-1 suppresses expression of genes involved in mouse and human TNF signaling. A, Colitis was induced in RAG KO mice by adoptive transfer of CD4<sup>+</sup> CD25<sup>-</sup> T cells on day 0. Mice received PBS or *Na*-AIP-1 twice per week by intraperitoneal injection. Termination was conducted at day 27, when all vehicle control (PBS) mice displayed clinical indicators of colitis. RNA-seq was conducted on distal colon sections and transcriptomic expression profiles of genes involved in TNF signaling (KEGG) were analyzed. Forty-three genes in this pathway underwent significant downregulation when log<sub>2</sub> fold-change was analyzed using EDGE\_R. Heatmap was generated using Graphpad Prism 8. B, Human THP-1 derived M1 macrophages were stimulated for 24 hours with 10 ng/mL LPS in the presence of PBS (vehicle control, black bar) or 100  $\mu$ g/mL *Na*-AIP-1 (grey bar). TNF release was analysed using the Legendplex assay. Each symbol represents a technical replicate. Data from one experiment is shown, and a second independent experiment analysed by ELISA resulted in a similar outcome. \*\*\* *P* < 0.001 (unpaired t test).

human tissue, recombinant *Na*-AIP-1 was co-cultured with human THP-1 derived M1 macrophages for 24 h with LPS in the presence of PBS vehicle or recombinant *Na*-AIP-1. In 2 separate experiments, significant suppression of TNF release was detected using both the Legendplex assay and ELISA (*P* < 0.001) using an unpaired *t* test (Fig 6, B).

## DISCUSSION

As the burden of conditions driven by inappropriate immune responses continues to grow, the need for effective therapeutic interventions has become more critical. The unique symbiotic relationship shared between human and helminth has presented the opportunity for the discovery of a pharmacopoeia of novel biologics, which come with the advantage of a favorable tolerability profile afforded by centuries of host-parasite co-evolution. *N. americanus*, in particular, is exquisitely well adapted to reside within the human gut for several years, without instigating the inflammatory response anticipated against a pathogen. Herein we describe 2 TIMP-like proteins in the *N. americanus* secretome, both notable for their homology to molecules responsible for the regulation of chronic and acute inflammation in several mammalian species, including humans. One of these proteins, subsequently named *Na-AIP-1*, displayed potent immunomodulatory properties in suppressing inflammatory pathology in distinct murine models of colitis, as well as *ex vivo* suppression of TNF signaling in a human M1 macrophage cell line.

In the TNBS-induced model of acute chemically-induced colitis, prophylactic i.p. delivery of *Na-AIP-1* protected against inflammatory pathology. This was demonstrated across immunologically distinct murine strains, where efficacy is most apparent when *Na-AIP-1* is provided prior to disease onset, since administration of *Na-AIP-1* after TNBS administration had limited efficacy. Together, these findings suggest that *Na-AIP-1* may be more suited as a preventative treatment for colitis, or as a maintenance therapy to prevent disease reactivation. The prophylactic efficacy of *Na-AIP-1* appears to be dependent on the presence of CD11c+ cells, similar to what has been reported for a related hookworm-secreted protein *Ac-AIP-2* in an asthma model.<sup>13</sup> The precise mechanisms by which *Na-AIP-1* acts via CD11c+ cells to exert its immunomodulatory effects remain undefined, and further studies are required to determine if *Na-AIP-1* induces tolerogenic DC populations, similar to *Ac-AIP-2*, as well as the action of other CD11c+ cells such as macrophages.

In the T cell transfer model of murine colitis, prophylactic delivery of *Na-AIP-1* was similarly able to curtail inflammation and reduce the presence of inflammatory CD4+ T cells in the colon. Transcriptional profiling of the colon tissue-specific immunomodulatory response induced by *Na-AIP-1* in the T cell transfer colitis model revealed multiple anti-inflammatory biological pathways that are shared with anti-IL-12/23p40 mAb treatment. However, *Na-AIP-1* appeared to uniquely influence several biological processes,

including the upregulation of steroid hormone biosynthesis and fatty acid metabolism, and the suppression of NK cell-mediated cytotoxicity (granzymes primarily) and inflammatory cytokine signaling pathways. Patients with UC display high levels of granzyme M (GrzM) mRNA in inflamed colon tissue.<sup>47</sup> Moreover, granzyme B-expressing mucosal B cells were more prominent in CD and UC patients compared to normal gut intestinal mucosa,<sup>48</sup> suggestive of a role for these cells in IBD-dependent epithelial damage. While a direct link to NK cells has not yet been established, *Na-AIP-1* might act directly on NK cells, or indeed other granzyme-secreting cells, to suppress their cytotoxic properties, and this warrants exploration in the future.

The expectation was that *Na-AIP-1* would act similarly to netrin domain-containing homologs isolated and cloned from the secretions of canine hookworms, and induce a proregulatory immune environment. Navarro et al<sup>13</sup> described a mechanism by which i.p. administration of *Ac-AIP-2* led to an expansion in CD11c+ DC populations in mesenteric lymph nodes, correlating with an increase in tolerance-inducing retinaldehyde dehydrogenase activity. Treatment with *Ac-AIP-2* was also associated with an increase in FoxP3+ T<sub>REG</sub> cell populations at mucosal sites, and a reduction in proinflammatory cytokines. Similarly, Ferreira et al<sup>26</sup> demonstrated suppression of Th1/Th17-associated cytokines in TNBS-induced colitis following *Ac-AIP-1* treatment, as well as an upregulation in IL-10 accompanying increased proliferation of T<sub>REG</sub> cells in the colon at termination. Herein, *Na-AIP-1* was also able to potently suppress proinflammatory Th1 cytokines, including TNF, and minimize inflammatory pathology in both colitis models; yet, some inconsistencies emerged in the effects of these two proteins on leukocyte populations. While we did not quantify T<sub>REG</sub> populations in the TNBS-induced colitis studies included herein, *FoxP3* transcription was not enhanced in the intestinal transcriptome of *Na-AIP-1*-treated RAG KO mice 27 days after receiving adoptive transfer of CD4+ CD25- T cells, despite the mice being protected against colitis. However, the duration of the adoptive transfer model must also be considered; it is possible that T<sub>REG</sub> proliferation may have occurred earlier in the progression of the disease, which had since subsided. Further research is required to determine whether the mechanism of immunosuppression of *Na-AIP-1* is associated with promotion of T<sub>REG</sub> responses, or is dependent on other mechanisms.

What little is understood regarding this family of unique molecules seemingly confounds expectations based on current information; to our knowledge, they remain the only N-terminal netrin domain bearing



proteins which have been identified outside of mammalian TIMPs, to which they display a high level of sequence conservation, and similarly modulate inflammation. Yet, helminth-derived TIMP-like proteins show no evidence of MMP binding or inhibition in the exertion of their anti-inflammatory effect. A comprehensive characterization of the crystal structure of *Ancylostoma ceylanicum* AceES-2 confirmed the TIMP-like homology of the N-terminal netrin domain, but recombinant AceES-2 did not inhibit any of the 10 most abundant human MMPs.<sup>23</sup> Moreover, the authors concluded that the structure of AceES-2 prevented access of the N-terminus of the protein to the active site cleft of MMPs, and therefore the protein was highly unlikely to function as a true TIMP. An additional level of complexity is added when considering NECAME\_13168; despite a high level of homology with *Na*-AIP-1 and a similar elevated transcription during the infectious stage of the parasitic life cycle, recombinant NECAME\_13168 did not display anti-inflammatory properties, suggesting either no immunomodulatory influence, or a potential lack of suitability for recombinant production in the *P. pastoris* system. The likely physiological role of NECAME\_13168 remains unclear at this stage, and potentially in contradiction to other TIMP-like hookworm proteins. However, identification of sequence or morphological divergences from *Na*-AIP-1, *Ac*-AIP-1 and *Ac*-AIP-2 may assist in the determination of regions contributing to anti-inflammatory activity.

Our findings demonstrate the prophylactic efficacy of recombinantly produced *Na*-AIP-1 in the amelioration of clinical and histological indicators of colitis in 2 distinct murine models of IBD. In the chemically-induced TNBS model of acute colitis, this effect is dependent on the presence of CD11c+ APCs. In the CD4+ CD25- adoptive transfer-induced model of chronic colitis, where inflammation is instigated by a disruption in T cell homeostasis, prophylactic administration of *Na*-AIP-1 induces a transcriptomic profile that correlates with a downregulation in metabolic and signaling pathways associated with Th1 inflammation. Whether *Na*-AIP-1 exhibits therapeutic efficacy at limiting active disease in this model was not determined, and should be the subject of future investigation. Further, it is unclear if the choice of the CD4+ CD25- model of T-cell transfer colitis may have affected the experimental outcomes, due to the heterogeneous nature of the transferred T cells. Future studies could investigate the efficacy of *Na*-AIP-1 in the more widely published CD45RBhi T cell transfer model,<sup>49</sup> where pure populations of naïve T cells are transferred, which may provide additional insight into the cellular mechanisms of how *Na*-AIP-1 suppresses colitis. While the

elucidation of the molecular mechanism remains elusive, *Na*-AIP-1 nonetheless presents as an excellent candidate for further clinical development. Suppression of TNF secretion by human THP-1-derived M1 macrophages is encouraging and suggests that the anticolic properties of *Na*-AIP-1 in mice might indeed translate into human IBD. The identification of binding partners and the characterization of the pharmacokinetics involved in *Na*-AIP-1 metabolism are fundamental in the determination of its potential for development as a novel biologic. Future work should further explore the impact of *Na*-AIP-1 on human tissues *ex vivo*, including APCs from gut biopsies of IBD patients.

Whilst several studies have been published detailing the potential of hookworm-derived products in the TNBS and DSS models of murine colitis,<sup>26,50,51</sup> this is the first report of the prophylactic efficacy of a helminth-secreted protein in the robust murine T cell transfer model of colitis, which closely resembles human disease. Further, the discovery of a potential anti-inflammatory therapeutic from an anthropophilic parasite like the human hookworm *N. americanus*, as well as *ex vivo* bioactivity with a human macrophage cell line, may favor a greater safety profile if eventually translated to humans as a maintenance or preventative therapy. As such the studies contained within represent an exciting progression in development of helminth ES products as human biologics.

#### ACKNOWLEDGMENTS

All authors have read the journal's authorship agreement. This work was supported by the National Health and Medical Research Council (NHMRC) through a program grant (1132975) and senior principal research fellowship (1117504) to A.L., an Advance Queensland fellowship to P.G., Paragen Bio research contract to A. L., P.G. and N.D., a research contract from Janssen R&D, an Australian Postgraduate Award to G.B., and an Australian Research Council Special Research Initiative award to the Australian Institute of Tropical Health and Medicine at James Cook University (SRI40200003). The funders had no role in study design, data collection and analysis, decision to publish, or preparation of the manuscript. All authors have read the journal's policy on disclosure of potential financial and personal conflicts of interest and there are none to report.

#### SUPPLEMENTARY MATERIALS

Supplementary material associated with this article can be found in the online version at doi:[10.1016/j.trsl.2021.02.012](https://doi.org/10.1016/j.trsl.2021.02.012).

REFERENCES

- Molodecky NA, Soon IS, Rabi DM, et al. increasing incidence and prevalence of the inflammatory bowel diseases with time, based on systematic review. *Gastroenterology* 2012;142:46–54.
- Bager P, Arved J, Rønborg S, et al. *Trichuris suis* ova therapy for allergic rhinitis: a randomized, double-blind, placebo-controlled clinical trial. *J Allerg Clin Immunol* 2010;125:123–30.
- Mizoguchi A. Animal models of inflammatory bowel disease. *Prog Mol Biol Transl Sci* 2012;105:263–320.
- Croese J, Giacomini P, Navarro S, et al. Experimental hookworm infection and gluten microchallenge promote tolerance in celiac disease. *J Allerg Clin Immunol* 2015;135:508–16.
- Croese J, O’Neil J, Masson J, et al. *A proof of concept study establishing Necator americanus in Crohn’s patients and reservoir donors*. *Gut* 2006;55:136–7.
- Summers RW, Elliott DE, Urban JF Jr., Thompson RA, Weinstock JV. *Trichuris suis* therapy for active ulcerative colitis: a randomized controlled trial. *Gastroenterol* 2005;128:825–32.
- Garg SK, Croft AM, Bager P. Helminth therapy (worms) for induction of remission in inflammatory bowel disease. *Cochrane Data Syst Rev* 2014;Cd009400. doi: 10.1002/14651858.CD009400.pub2.
- Ryan SM, Eichenberger RM, Ruscher R, Giacomini PR, Loukas A. Harnessing helminth-driven immunoregulation in the search for novel therapeutic modalities. *PLoS Path* 2020;16:e1008508.
- Maizels RM, Smits HH, McSorley HJ. Modulation of host immunity by helminths: the expanding repertoire of parasite effector molecules. *Immunity*. 2018;49:801–18.
- Ruysers NE, De Winter BY, De Man JG, et al. Therapeutic potential of helminth soluble proteins in TNBS-induced colitis in mice. *Inflamm Bowel Dis* 2009;15:491–500.
- Cançado GGL, Fiuza JA, de Paiva NCN, et al. Hookworm products ameliorate dextran sodium sulfate-induced colitis in BALB/c mice. *Inflamm Bowel Dis* 2011;17:2275–86.
- Ferreira I, Smyth D, Gaze S, et al. Hookworm excretory/secretory products induce interleukin-4 (IL-4) IL-10 CD4 T cell responses and suppress pathology in a mouse model of colitis. *Infect Immun* 2013;81:2104–11.
- Navarro S, Pickering DA, Ferreira IB, et al. Hookworm recombinant protein promotes regulatory T cell responses that suppress experimental asthma. *Sci Transl Med* 2016;8:362ra143.
- Cantacessi C, Mitreva M, Jex AR, et al. Massively parallel sequencing and analysis of the *Necator americanus* transcriptome. *PLoS Negl Trop Dis* 2010;4:e684.
- Wang Z, Abubucker S, Martin J, Wilson R, Hawdon J, Mitreva M. Characterizing *Ancylostoma caninum* transcriptome and exploring nematode parasitic adaptation. *BMC Genomics* 2010;11:1–19.
- Schwarz EM, Hu Y, Antoshechkin I, Miller MM, Sternberg PW, Aroian RV. The genome and transcriptome of the zoonotic hookworm *Ancylostoma ceylanicum* identify infection-specific gene families. *Nature Genet* 2015;47:416–22.
- Tang YT, Gao X, Rosa BA, et al. Genome of the human hookworm *Necator americanus*. *Nature Genet* 2014;46:261–9.
- Zhan B, Badamchian M, Meihua B, et al. Molecular cloning and purification of Ac-TMP, a developmentally regulated putative tissue inhibitor of metalloprotease released in relative abundance by adult *Ancylostoma* hookworms. *Am J Trop Med Hyg* 2002;66:238–44.
- Zhan B, Gupta R, Wong SPY, et al. Molecular cloning and characterization of Ac-TMP-2, a tissue inhibitor of metalloproteinase secreted by adult *Ancylostoma caninum*. *Mol Biochem Parasitol* 2008;162:142–8.
- Mulvenna J, Hamilton B, Nagaraj SH, Smyth D, Loukas A, Gorman JJ. Proteomics analysis of the excretory/secretory component of the blood-feeding stage of the hookworm, *Ancylostoma caninum*. *Mol Cell Proteomics* 2009;8:109–21.
- Morante T, Shepherd C, Constantinoiu C, Loukas A, Sotillo J. Revisiting the *Ancylostoma caninum* secretome provides new information on hookworm-host interactions. *Proteomics* 2017;17:23–4.
- Banyai L, Patthy L. The NTR module: domains of netrins, secreted frizzled related proteins, and type I procollagen C-proteinase enhancer protein are homologous with tissue inhibitors of metalloproteases. *Protein Sci* 1999;8:1636–42.
- Kucera K, Harrison LM, Cappello M, Modis Y. *Ancylostoma ceylanicum* excretory-secretory protein 2 adopts a netrin-like fold and defines a novel family of nematode proteins. *J Mol Biol* 2011;408:9–17.
- Cantacessi C, Hofmann A, Pickering D, Navarro S, Mitreva M, Loukas A. TIMPs of parasitic helminths - a large-scale analysis of high-throughput sequence datasets. *Parasit* 2013;6:156.
- Bruikman CS, Zhang H, Kemper AM, van Gils JM. Netrin family: role for protein isoforms in cancer. *J Nucl Acids* 2019;3947123. <https://doi.org/10.1155/2019/3947123>.
- Ferreira IB, Pickering DA, Troy S, Croese J, Loukas A, Navarro S. Suppression of inflammation and tissue damage by a hookworm recombinant protein in experimental colitis. *Clin Transl Immunol* 2017;6:e157.
- Koradi R, Billeter M, Wüthrich K. MOLMOL: a program for display and analysis of macromolecular structures. *J Mol Graph* 1996;14:51–5.
- Yang J, Yan R, Roy A, Xu D, Poisson J, Zhang Y. The I-TASSER Suite: protein structure and function prediction. *Nature Meth* 2015;12:7–8.
- Cobos Caceres C, Bansal PS, Navarro S, et al. An engineered cyclic peptide alleviates symptoms of inflammation in a murine model of inflammatory bowel disease. *J Biol Chem* 2017;292:10288–94.
- Ostanin DV, Bao J, Koboziev I, et al. T cell transfer model of chronic colitis: concepts, considerations, and tricks of the trade. *Am J Physiol Gastro Liver Physiol* 2009;296:135–46.
- Weigmann B. Induction of colitis in mice (T-cell transfer model). *Meths Mol Biol* 2014;1193:143–51.
- Anderson CA, Boucher G, Lees CW, et al. Meta-analysis identifies 29 additional ulcerative colitis risk loci, increasing the number of confirmed associations to 47. *Nature Genet* 2011;43:246–52.
- Dobin A, Davis CA, Schlesinger F, et al. STAR: ultrafast universal RNA-seq aligner. *Bioinformatics* 2013;29:15–21.
- Risso D, Schwartz K, Sherlock G, Dudoit S. GC-content normalization for RNA-Seq data. *BMC Bioinform* 2011;12:480.
- Risso D, Ngai J, Speed TP, Dudoit S. Normalization of RNA-seq data using factor analysis of control genes or samples. *Nature Biotechnol* 2014;32:896–902.
- Waardenberg AJ, Field MA. consensusDE: an R package for assessing consensus of multiple RNA-seq algorithms with RUV correction. *PeerJ* 2019;7:e8206.
- McCarthy DJ, Chen Y, Smyth GK. Differential expression analysis of multifactor RNA-Seq experiments with respect to biological variation. *Nucl Acids Res* 2012;40:4288–97.
- Robinson MD, McCarthy DJ, Smyth GK. edgeR: a Bioconductor package for differential expression analysis of digital gene expression data. *Bioinformatics* 2010;26:139–40.
- Chanput W, Mes JJ, Savelkoul HF, Wichers HJ. Characterization of polarized THP-1 macrophages and polarizing ability of LPS and food compounds. *Food Function* 2013;4:266–76.
- Abad C, Martinez C, Juarranz MG, et al. Therapeutic effects of vasoactive intestinal peptide in the trinitrobenzene sulfonic acid mice model of Crohn’s disease. *Gastroenterol* 2003;124:961–71.
- Antonioni E, Margonis GA, Angelou A, et al. The TNBS-induced colitis animal model: an overview. *Annals Med Surg* 2016;11:9–15.

42. MacDonald JK, Nguyen TM, Khanna R, Timmer A. Anti-IL-12/23p40 antibodies for induction of remission in Crohn's disease. *Cochrane Database Syst Rev* 2016;11:Cd007572.
43. Lindebo Holm T, Poulsen SS, Markholst H, Reedtz-Runge S. Pharmacological evaluation of the SCID T cell transfer model of colitis: as a model of Crohn's disease. *Int J Inflamm* 2012;2012:412178.
44. Kjellef S, Lundsgaard D, Poulsen SS, Markholst H. Reconstitution of Scid mice with CD4+CD25- T cells leads to rapid colitis: an improved model for pharmacologic testing. *Int Immunopharmacol* 2006;6:1341–54.
45. Pan W, Zhu S, Dai D, et al. MiR-125a targets effector programs to stabilize Treg-mediated immune homeostasis. *Nature Comm* 2015;6:7096.
46. Metwali A, Winckler S, Urban JF Jr., Kaplan MH, Ince MN, Elliott DE. Helminth-induced regulation of T-cell transfer colitis requires intact and regulated T cell Stat6 signaling in mice. *Eur J Immunol* 2020. <https://doi.org/10.1002/eji.201848072>.
47. Souza-Fonseca-Guimaraes F, Krasnova Y, Putoczki T, et al. Granzyme M has a critical role in providing innate immune protection in ulcerative colitis. *Cell Death Dis* 2016;7:e2302.
48. Cupi ML, Sarra M, Marafini I, et al. Plasma cells in the mucosa of patients with inflammatory bowel disease produce granzyme B and possess cytotoxic activities. *J Immunol* 2014;192:6083–91.
49. Shale M, Schiering C, Powrie F. CD4(+) T-cell subsets in intestinal inflammation. *Immunol Rev* 2013;252:164–82.
50. Eichenberger RM, Ryan S, Jones L, et al. Hookworm secreted extracellular vesicles interact with host cells and prevent inducible colitis in mice. *Front Immunol* 2018;9:850.
51. Wangchuk P, Shepherd C, Constantinoiu C, et al. Hookworm-derived metabolites suppress pathology in a mouse model of colitis and inhibit secretion of key inflammatory cytokines in primary human leukocytes. *Infect Immun* 2019;87(4):e00851-18.